Insights into the structure of human cytomegalovirus large terminase subunit pUL56

Christos G.W. Savva[a], Andreas Holzenburg[a,b,1], Elke Bogner[c,1,*]

[a] *Microscopy and Imaging Center, Department of Biology, Texas A&M University, College Station, TX 77843-2257, USA*
[b] *Department of Biochemistry and Biophysics, Texas A&M University, College Station, TX 77843-2257, USA*
[c] *Institut für Klinische und Molekulare Virologie, Schlossgarten 4, D-91054 Erlangen, Germany*

Received 20 January 2004; revised 19 February 2004; accepted 10 March 2004

First published online 18 March 2004

Edited by Hans-Dieter Klenk

Abstract Terminases are a class of proteins which catalyze the generation of unit-length genomes during DNA packaging. These essential proteins are conserved throughout the herpesviruses and many double-stranded DNA bacteriophages. We have determined the structure of the large terminase subunit pUL56 of human cytomegalovirus, a highly pathogenic virus, to 2.6 nm resolution. Image analysis of purified pUL56 suggests that the molecule exists as a dimer formed by the association of two ring-like structures positioned on top of each other and connected by a pronounced density on one side. The 3D reconstruction of pUL56 provides first structural insights into the active protein.

Key words: Human cytomegalovirus; DNA packaging; Terminase; Three-dimensional structure

1. Introduction

Human cytomegalovirus (HCMV), one of eight human herpesviruses, can cause life-threatening diseases. 40–80% of the human population are infected prior to adulthood. In neonates as well as in immunocompromised adults HCMV is a serious pathogen that can cause fatal organ damage [1].

DNA packaging is the key step in viral maturation and involves binding and cleavage of viral DNA containing specific DNA-packaging motifs. This is a common feature for many double-stranded DNA bacteriophages and herpesviruses. Viral DNA replication leads to the formation of concatemeric DNA which must be resolved into unit-length genomes during packaging. The subsequent packaging process requires for some bacteriophages and herpesviruses site-specific cleavage at *pac* motifs located within the *a* sequence of the terminal and internal repeat segments [2–8]. Unit-length genomes are then encapsidated into preassembled capsids/proheads. This process is mediated by a group of specific enzymes called terminases. Terminases catalyze the ATP-dependent translocation of viral DNA into the procapsids as well as cleavage of concatenated DNA [9,10]. Most terminases are hetero-oligomers with each subunit carrying a different function [11–16]. Mutations in any of the encoding genes lead to an accumulation of empty procapsids/proheads and uncleaved concatemeric DNA in the nucleus [9,17,18]. Our previous data together with the reports from Krosky et al. [19] and Underwood et al. [20] indicated that the terminase of HCMV consists of the highly conserved proteins pUL56 and pUL89 [21–26]. Since viral DNA packaging and cleavage into unit-length genomes is one of the first processes during viral assembly, a terminase inhibitor would block the formation of new virions at an early stage. pUL56 and/or pUL89 are attractive drug targets since mammalian cell DNA replication does not involve cleavage of concatemeric DNA. In this connection it is interesting to note that two compounds targeting pUL56 and pUL89, BAY 38-4766 and 2-bromo-5,6-dichloro-1-β-D-ribofuranosyl benzimidazole (BDCRB)-derived GW273175X, have completed or entered phase I clinical trials. Both compounds were very successful, but clinical development of both has been halted [27].

Despite the importance of these proteins and intensive research into biochemical and functional aspects of terminases, there is still a lack of structural information. This is mainly due to the extremely small quantities of protein available, which limit X-ray crystallographic analysis. In contrast to this, three-dimensional (3D) reconstruction by single particle analysis can be performed with picomole amounts of protein. Previously we demonstrated that single particles of purified terminase subunits pUL56 and pUL89 occurred as a distinct ring-shaped structure as revealed by single particle electron microscopy [25]. Here we present a detailed structural analysis of the large terminase subunit pUL56. The 3D reconstruction to 2.6 nm resolution represents the first 3D structure of a large terminase subunit and allows a first insight into the structure–function relationships of this important viral enzyme system.

2. Materials and methods

2.1. Cells and viruses

Insect cells 5B1-4 (High five) were grown in TC-100 medium supplemented with 10% fetal calf serum, glutamine and gentamicin (60 μg/ml) [28]. For generation of recombinant baculovirus transposition into the bacmid bMON14272 was used as described by Luckow et al. [29]

2.2. Purification of the large terminase subunit pUL56

For protein purification High five cells (7×10^7) expressing the recombinant pUL56 were harvested 48 h post infection. Purification protocols were performed as described before [25]. In general lysed cells were subjected to two-step purification by chromatography. The first is an anion exchange chromatography with a Resource Q™ column (Amersham Bioscience), followed by size exclusion chromatog-

*Corresponding author. Fax: (49)-9131-8526493.
E-mail address: eebogner@viro.med.uni-erlangen.de (E. Bogner).

[1] Equal senior authors.

0014-5793/04/$30.00
doi:10.1016/S0014-5793(04)00283-2

raphy using a HiPrep 16/60 Sephacryl™ S-300 HR gel permeation column. The fractions containing the protein were pooled and spin-concentrated on a PES membrane (type Spin-MICRO) with a 30 kDa cut-off (membraPure, Bodenheim, Germany), aliquoted and stored at −80°C.

2.3. Bioluminometric ATPase activity assay

Purified rpUL56 (0.3 μg), extracts from insect cells (High five) or apyrase (EC 3.6.1.5) were incubated in 200 μl of ATPase buffer (100 mM Tris-acetate, pH 7.5, 2 mM EDTA, 10 mM magnesium acetate, 0.1% bovine serum albumin, 1 mM dithiothreitol) containing 20 μg D-luciferin and 1 ng luciferase. The samples were incubated at 30°C for 30 min. The luminescence was measured in a microplate luminometer (OrionII, Berthold Detection Systems, Germany). By using the software Simplicity™ the measurement parameters were defined (fast kinetics, measurement time 40 s) and the reaction was initiated by injection of 40 μl of 0.2 pmol ATP. The results were displayed on the screen and the data exported directly into Excel™. This assay allows a direct measurement of the ATP hydrolysis of the proteins by the amount of decreasing ATP.

2.4. Protein/protein interaction by chemical cross-linking

Glutathione *S*-transferase (GST)-UL56 (300 ng) were incubated for 5 min at room temperature in phosphate-buffered saline in a final volume of 20 μl. The cross-linking reaction was started by addition of 0.1% glutaraldehyde to a final concentration of 0.01%. The reaction was stopped by addition of 10 μl sodium dodecyl sulfate (SDS) loading buffer and denaturation of the samples for 2 min at 95°C. The proteins were separated by 8% SDS–polyacrylamide gel electrophoresis (PAGE) and analyzed by Western blot with the monospecific antibody pAbUL56.

2.5. Western blot

The fractions were separated on 8% (w/v) native polyacrylamide gel, transferred to nitrocellulose sheets and subjected to Western blot analysis as described previously [16]. The antibody pAbUL56 (1:10 [16]) specific for pUL56 was used as primary antibody prior to incubation with horseradish peroxidase-conjugated anti-human $F(ab')_2$ fragments (1:1000 in milk powder).

2.6. Electron microscopy

Negatively stained specimens of purified protein were prepared essentially according to Valentine et al. [30] using an aqueous solution of uranyl acetate (4% (w/v), pH 4.3) and omitting any fixation steps. Specimens were mounted onto 400 mesh copper grids and observed in a Zeiss EM T109 operated at an acceleration voltage of 80 kV. Electron micrographs were recorded at a calibrated magnification (29 600×). DNA–protein complexes were prepared by incubating the purified protein rpUL56 (1 μg) with linearized DNA (0.2 μg) containing the *a* sequence (30 min at 30°C) in a final volume of 50 μl HEPES buffer (20 mM, pH 7.4) and a molar ratio of protein:DNA of 1:4. The formed complexes were fixed with glutaraldehyde by adding 1.25 μl of an 8% (v/v) freshly prepared solution in distilled water and incubating for 10 min. Specimens were mounted onto freshly glow-discharged carbon-coated copper grids (400 mesh) and incubated for 60 s prior to staining with uranyl acetate.

2.7. Image analysis and 3D reconstruction

Selected electron micrographs were digitized using a LeafScan 45 microdensitometer. Scanning increments were adjusted so that the final scan step of 20 μm corresponded to 0.67 nm/pixel at the specimen level. Particle selection and particle averaging was performed by using IMAGIC-5 [31] and EMAN [32] software packages running on a Pentium PC under Linux. Micrograph quality was assessed by examining the average power spectrum of a set of particles selected from each micrograph. Images were then bandpass-filtered and aligned by reference-free alignment [33]. Three main classes of projections were determined by multivariate statistical analysis and hierarchical ascendant classification with complete linkage. Resolution was assessed by using the standard Fourier shell correlation criterion [34,35]. The angular refinement process was stopped after five iterations, when no further increase of resolution was observed. The 3D reconstructions of pUL56 were visualized using VIS5D and VMD [36]. The threshold level of the surface was set to include a volume corresponding to 187 kDa, assuming a protein density of 1.37 $Å^3$/Da [37]. Fourier shell correlation indicated a resolution of 2.6 nm.

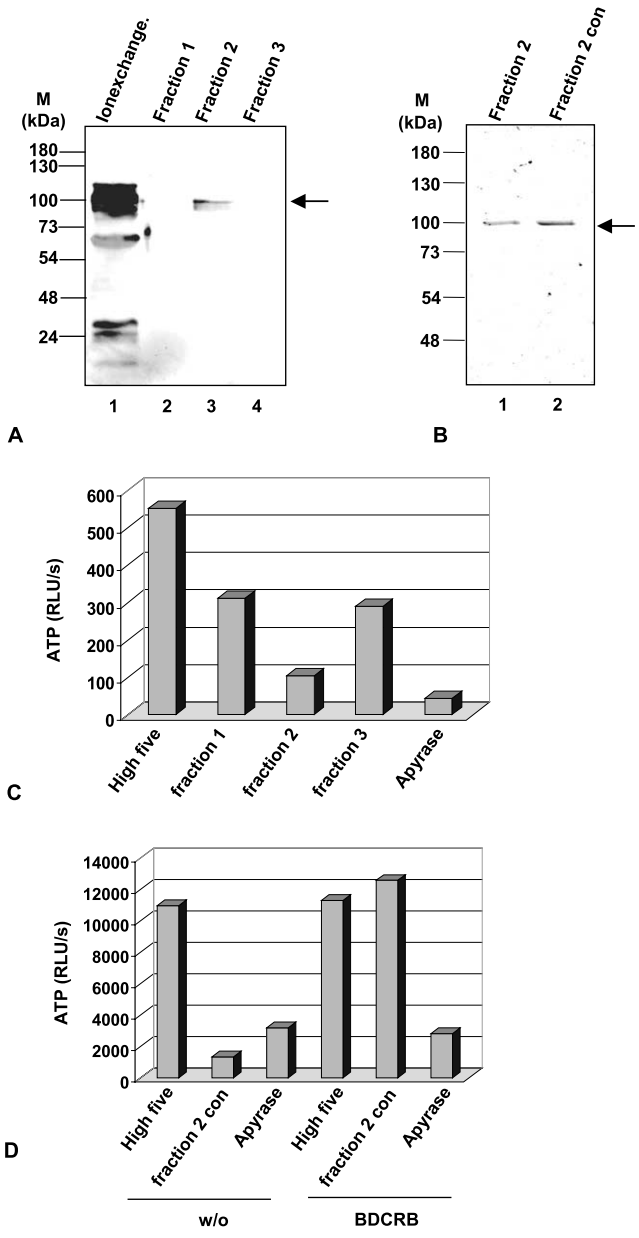

Fig. 1. Analysis of purified rpUL56 and direct association with enzyme activity. A: Aliquots after ion exchange (ionexchange) and gel permeation chromatography (fractions 1–3) were subjected to SDS–PAGE prior to Western blot with monospecific pAbUL56. Molecular weight markers (M) are indicated on the left; position of the protein is indicated by an arrow. B: Aliquots after purification (Fraction 2) and following spin concentration (Fraction 2 con) were subjected to SDS–PAGE prior to staining with Coomassie. Molecular weight markers (M) are indicated on the left; position of the protein is indicated on the right. C: ATPase activity of the purified protein. Extracts from High five cells (High five), fractions after gel permeation chromatography (fractions 1–3) and apyrase were preincubated in the assay mixture before the reaction was started by addition of ATP. The degradation of ATP was detected by the luciferase system. D: Specificity of the enzyme activity. Apyrase as well as Fraction 2 con were preincubated with BDCRB in the reaction mixture. The reaction was started by addition of ATP followed by detection of ATP hydrolysis using the luciferase system.

3. Results

3.1. Purification of the rpUL56

To obtain further insights into the structure we first purified recombinant baculovirus-pUL56-infected cell extracts with anion exchange chromatography followed by gel permeation chromatography. Aliquots of the rpUL56-containing fraction after ion exchange and three fractions after gel permeation chromatography were assayed for protein content by SDS–PAGE followed by transfer to nitrocellulose. The nitrocellulose filters were reacted with the affinity-purified antibody against pUL56, pAbUL56. Fraction 2 containing rpUL56 (Fig. 1A) was used for further analysis. The purity of Fraction 2 was demonstrated by SDS–PAGE prior to Coomassie staining (Fig. 1B, lane 1). The fraction was also homogeneous after spin concentration (Fig. 1B, Fraction 2 con). Positions of rpUL56 are indicated by arrows, molecular weight standards are indicated on the left side.

3.2. ATPase activity of purified rpUL56

In order to determine whether the protein is active, the capacity to hydrolyze ATP was analyzed by real-time ATPase activity assays according to Karamohamed and Guidotti [38]. This method enables a continuous monitoring of ATP hydrolysis by combining the enzyme activity of proteins with the firefly luciferase system. The purified proteins were incubated with the reaction mixture prior to addition of ATP for starting the reaction. The fraction containing the purified rpUL56 as well as *Apyrase* (EC 3.6.1.5) showed a decrease of ATP concentration (Fig. 1C, Fraction 2, Apyrase). Extracts from insect cells were used as control reactions (Fig. 1C, High five).

3.3. Inhibition of the ATPase activity by BDCRB

To demonstrate the specificity of the enzyme activity of rpUL56 experiments were carried out in the presence of BDCRB. While BDCRB had no effect on the enzyme activity of *Apyrase*, enzymatic activity of rpUL56 in the presence of 125 μM BDCRB was completely inhibited (Fig. 1D, Fraction 2 con), thus demonstrating that purified rpUL56 is in its biologically active form and ready for further analysis.

Taken together, these results indicate that the purified

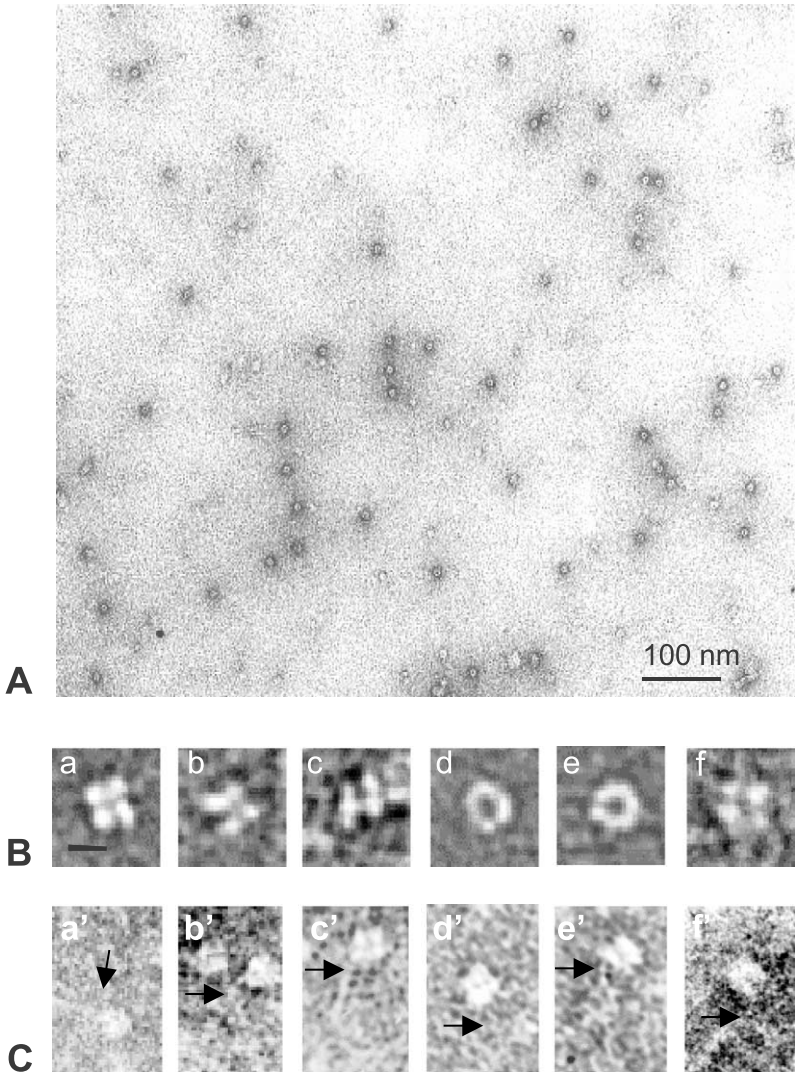

Fig. 2. Electron micrographs of negatively stained pUL56. A: Typical overview. B: Galleries showing different projections (including side-on views; a–c, f) in the absence of DNA and (C) after incubation with linear DNA containing an *a* sequence at the 5′ end. The bars in B and C correspond to 10 nm.

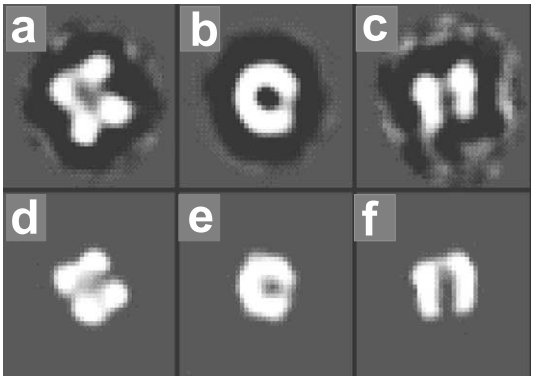

Fig. 3. Image analysis. a–c: Main rpUL56 class averages after multivariate statistical analysis represent square-shaped (a), ring-like (b) and U-shaped projections (c). The corresponding re-projections are shown in d–f. Box size is 27×27 nm.

rpUL56 is in its biologically active form and ready for further analysis.

3.4. Electron microscopy and structural determination

Negatively stained specimens of recombinant pUL56 in the absence of DNA were prepared essentially according to Valentine et al. [25] A representative overview is shown in Fig. 2A. Apart from the ring-like structures (face-on views; Fig. 2Bd,e) previously described [20], a smaller population of side-on views (Fig. 2Ba–c,f) were found that resembled side-on views noted in samples with DNA. Galleries of pUL56 in the absence and presence of DNA are shown in Fig. 2B,C, respectively.

Three-dimensional reconstruction was performed with images of pUL56 in the absence of DNA. The present structural study was accomplished using more than 1200 particles leading to a very robust reconstruction. At least three different projections can be discerned in the class averages, a ring-like face-on view, as well as U-shaped and square-shaped side-on views (Fig. 3a–c). These projections proved reproducible when re-projecting the 3D density distribution with the same mass threshold as used for surface rendering (Fig. 3d–f). The surface-rendered 3D reconstruction is characterized by two connected rings displaying a twofold axis parallel to the planes of the rings (C2 symmetry). Each ring measures about 9 nm in diameter and 2.5 nm in height and the central protein deficit is approximately 3.5 by 2.5 nm across (Fig. 4). It should be noted that each of the ring-like structures displays a density discontinuity opposite to the connection domain resulting in an almost two-pronged appearance that could endow the molecule with certain structural dynamics, like ring opening.

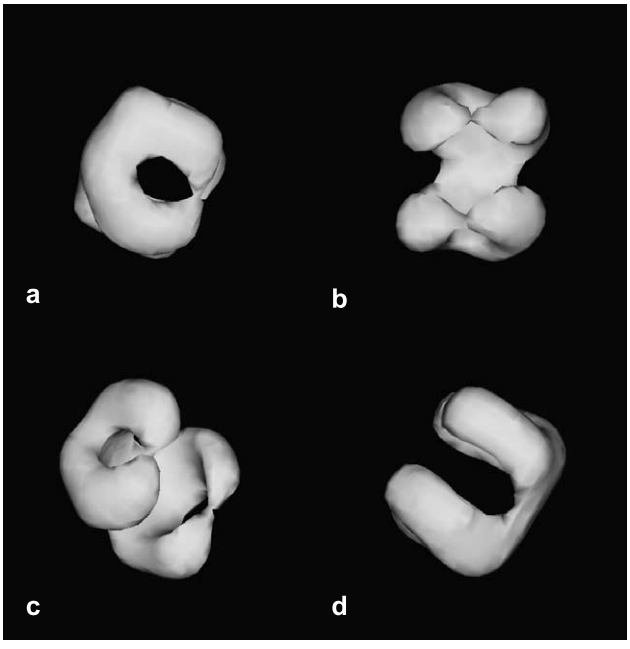

Fig. 4. Surface-rendered presentations of the pUL56 structure as determined by 3D reconstruction from single particles depicting pUL56 viewed face-on (a, displaying a typical ring-like appearance) and side-on (b, giving rise to the square-shaped projection; and d, the U-shaped projection). The presentation in c is obtained when tilting the ring-like view by 45°.

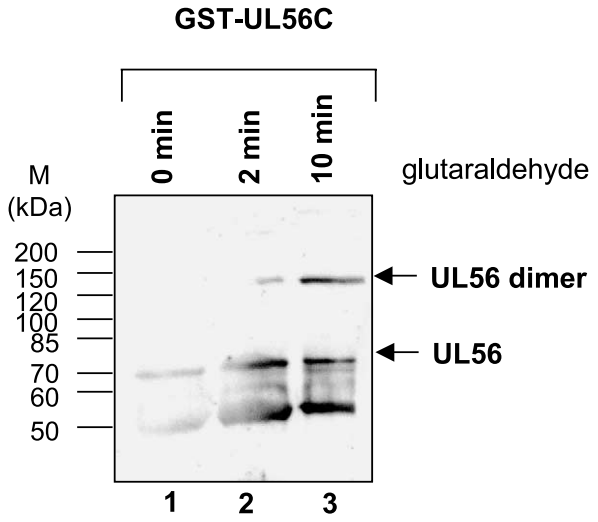

Fig. 5. Analysis of the association of pUL56 with itself by protein cross-linking. GST-UL56C was reacted with glutaraldehyde for the indicated times, followed by 8% SDS–PAGE and Western blot analysis. Molecular weight markers (M) are indicated on the left side; position of the protein is indicated on the right.

3.5. Interaction of pUL56 with itself

The interaction of pUL56 with itself was examined by chemical protein cross-linking. Purified GST-UL56C was treated for 0, 2 and 10 min with glutaraldehyde, before the proteins were separated by SDS–PAGE and analyzed by Western blot with monospecific antibody pAbUL56. A new protein band appeared, which corresponds to the GST-UL56C–GST-UL56C complex (Fig. 5). GST-UL56C formed a specific cross-linked complex with itself, implying its ability to form dimers.

4. Discussion

In this study we present, to our knowledge, the first 3D structure of the large terminase subunit pUL56 of HCMV revealing basic morphological signatures. Real-time ATPase activity assays demonstrated that the protein rpUL56 is in its active form and therefore suitable for structural analysis. Furthermore, the anti-HCMV agent BDCRB, recently shown to reduce the GST-UL56C ATPase activity [26], completely inhibited the enzyme activity of the full-length protein rpUL56. The observed ring-like projections together with

the side-on views which display two sets of densities related by a point of twofold rotational symmetry (Figs. 2B and 3) support the idea that pUL56 exists as a dimer. This finding is corroborated by 3D reconstructions using a density threshold corresponding to a monomer, i.e. 93 kDa. In such reconstructions the connectivity of protein densities is lost and the reprojections from the 3D structure do not resemble any of the class averages observed (data not shown). Mass–volume correlations have been successfully employed to establish the quaternary structure of macromolecular complexes [39–41]. In addition, if one expected a monomer, i.e. a single ring, side-on views would appear as thin rod-like structures measuring 2.5 nm across. Such projections were not present in the specimens.

Earlier observations showing that the *a* sequence was always located close to pUL56 molecules, displaying either a U-shaped or a square-shaped projection [25], suggest that the dimeric 3D structure represents pUL56 in the active state. It is also conceivable that upon binding of DNA containing one *a* sequence, the molecule (ring) opens up and that the protein domains involved in such dynamics would be candidates for housing the binding sites for DNA and ATP. Indirect supporting evidence is also gained from cross-linking analysis, which demonstrated that pUL56 can interact with itself, indicating the ability to form dimers. Comparable observations have been made with human topoisomerase I, which binds DNA in a central cavity upon ring opening followed by ring closing around the DNA [42], implying the existence of an 'open' configuration to initiate DNA binding. Recently, de Bear et al. [43] demonstrated by nuclear magnetic resonance analysis that the bacteriophage λ terminase subunit gpNu1 also forms dimers, a necessity for substrate binding. The DNA elements R2 and R3 are located on opposite sides to enable simultaneous binding and the architecture of *cos* motifs display an intrinsic bend between R2 and R3. Such features are not found in DNA containing *pac* motifs and therefore the mechanism for DNA binding by pUL56 is likely to be very different. In contrast to bacteriophages where both terminase subunits are non-structural proteins, HCMV pUL56 is a capsid-associated structural protein. Observations that pUL89 is never found together with pUL56 after DNA cleavage [25] support the idea that shortly after DNA cleavage into a unit-length genome, pUL89 is no longer associated with the DNA and recycled for further cleavage/packaging processes.

Further conclusions in terms of structure–function relationships of this key enzyme system of viral maturation must await higher resolution structural information on both pUL89 and pUL56.

Acknowledgements: We are grateful to J.C. Drach and L.W. Townsend (University of Michigan, Ann Arbor, MI, USA) for providing BDCRB. This work was supported in part by the Deutsche Forschungsgemeinschaft (Bo 1214/5-1). We thank B. Scholz for technical assistance and B. Fleckenstein for kind support.

References

[1] Alford, C.A. and Britt, W.J. (1993) in: The Human Herpesviruses (Roizman, B., Whitely, R.J. and Lopez, C., Eds.), pp. 227–255, Raven Press, New York.
[2] Adelman, K., Salmon, B. and Baines, J.D. (2001) Proc. Natl. Acad. Sci. USA 98, 3086–3091.
[3] Bogner, E. (2002) Rev. Med. Virol. 12, 109–129.
[4] Brown, J.C., McVoy, M.A. and Homa, F.L. (2002) in: Structure-Function Relationships of Human Pathogenic Viruses (Holzenburg, A. and Bogner, E., Eds.), pp. 111–153, Kluwer Academic/Plenum, New York.
[5] Chou, J. and Roizman, B. (1985) Cell 41, 803–811.
[6] Deiss, L.P., Chou, J. and Frenkel, N. (1986) J. Virol. 59, 605–618.
[7] Shibata, H., Fujisawa, H. and Minigawa, T. (1987) Virology 150, 250–258.
[8] Spaete, R.R. and Mocarski, E.S. (1985) J. Virol. 54, 817–824.
[9] Black, L.W. (1988) in: The Bacteriophages (Calendar, R., Ed.), pp. 321–373, Plenum, New York.
[10] Feiss, M. and Becker, A. (1983) in: Lambda II (Hendrix, R.W., Roberts, J.W., Stahl, F.W. and Weisberg, R.A., Eds.), pp. 305–330, Cold Spring Harbor Laboratory Press, Cold Spring Harbor, NY.
[11] Black, L.W., Showe, M.K. and Steven, A.C. (1994) in: Molecular Biology of Bacteriophage T4 (Karam, J., Drake, J.W., Kreuzer, K.N., Mosig, G., Hall, D.H., Eiserling, F.A., Black, L.W., Spicer, E.K., Kutter, E., Carlson, K. and Miller, E.S., Eds.), pp. 218–258, American Society for Microbiology, Washington, DC.
[12] Casjens, S. and Hendrix, R. (1988) in: The Bacteriophages (Calender, R., Ed.), pp. 15–19, Plenum, New York.
[13] Casjens, S. and Huang, W.M. (1982) J. Mol. Biol. 157, 287–298.
[14] Eppler, K., Wyckoff, E., Goates, J., Parr, R. and Casjens, S. (1991) Virology 183, 519–538.
[15] Fujisawa, H. and Hearin, P. (1994) Semin. Virol. 5, 5–13.
[16] Hendrix, R.W. and Garceao, R.L. (1994) Semin. Virol. 5, 15–26.
[17] Addison, C., Rixon, F.J. and Preston, V.G. (1990) J. Gen. Virol. 71, 2377–2384.
[18] Tengelsen, L.A., Pederson, N.E., Shaver, P.R., Wathen, M.W. and Homa, F.L. (1993) J. Virol. 67, 3470–3480.
[19] Krosky, P.M., Underwood, M.R., Turk, S.R., Feng, K.W-H., Jain, R.K., Ptak, R.G., Westerman, A.C., Biron, K.K., Townsend, L.B. and Drach, J.C. (1998) J. Virol. 72, 4721–4728.
[20] Underwood, M.R., Harvey, R.J., Stanat, S.C., Hemphill, M.L., Miller, T., Drach, J.C., Townsend, L.B. and Biron, K.K. (1998) J. Virol. 72, 717–722.
[21] Bogner, E., Reschke, M., Reis, M., Mockenhaupt, T. and Radsak, K. (1993) Virology 196, 290–293.
[22] Bogner, E., Radsak, K. and Stinski, M.F. (1998) J. Virol. 72, 2259–2264.
[23] Giesen, K., Radsak, K. and Bogner, E. (2000) FEBS Lett. 471, 215–218.
[24] Hwang, J.-S. and Bogner, E. (2002) J. Biol. Chem. 76, 1450–1460.
[25] Scheffczik, H., Savva, C.G.W., Holzenburg, A., Kolesnikova, L. and Bogner, E. (2002) Nucleic Acids Res. 30, 1695–1703.
[26] Scholz, B., Rechter, S., Drach, J.C., Townsend, L.B. and Bogner, E. (2003) Nucleic Acids Res. 31, 1426–1433.
[27] Wathen, M.W. (2002) Rev. Med. Virol. 12, 167–178.
[28] Summers, M.D. and Smith, G.E. (1987) A Manual of Methods for Baculovirus Vectors and Insect Cell Culture Procedures, Texas Agriculture Experiment Station, College Station, TX.
[29] Luckow, V.A., Lee, S.C., Barry, G.F. and Olins, P.O. (1993) J. Virol. 67, 4566–4579.
[30] Valentine, R., Shapiro, C. and Stadtman, E.R. (1968) Biochemistry 7, 2143–2152.
[31] van Heel, M., Harauz, G., Orlova, E.V., Schmidt, R. and Schatz, M. (1996) J. Struct. Biol. 116, 17–24.
[32] Ludtke, S.J., Baldwin, P.R. and Chiu, W. (1999) J. Struct. Biol. 128, 82–97.
[33] Penczek, P., Radermacher, M. and Frank, J. (1992) Ultramicroscopy 40, 33–53.
[34] Harrauz, G. and van Heel, M. (1986) Optik 73, 146–156.
[35] Saxton, W.O. and Baumeister, W. (1982) J. Microsc. 127, 127–138.
[36] Humphrey, W., Dalke, A. and Schulten, K. (1996) J. Mol. Graph. 14, 33–38.
[37] Zipper, P., Kratky, O., Herrmann, R. and Hohn, T. (1971) Eur. J. Biochem. 18, 1–9.
[38] Karamohamed, S. and Guidotti, G. (2001) BioTechniques 31, 420–425.

[39] Holzenburg, A., Bewley, M.C., Wilson, F.H., Nicholson, W.V. and Ford, R.C. (1993) Nature 363, 470–472.
[40] Sharma, S., Arockiasamy, A., Ronning, D.R., Savva, C.G.W., Holzenburg, A., Braunstein, M., Jacobs Jr., W.R. and Sacchettin, J.C. (2003) Proc. Natl. Acad. Sci. USA 100, 2243–2248.
[41] Wang, H.W., Chen, Y., Yang, H., Chen, X., Duan, M.X., Tai, P.C. and Sui, S.F. (2003) Proc. Natl. Acad. Sci. USA 100, 4221–4226.
[42] Stewart, L., Redinbo, M.R., Qiu, X., Hol, W.G.J. and Champoux, J. (1998) Science 279, 1534–1541.
[43] de Bear, T., Fang, J., Ortega, M., Yang, Q., Maes, L., Duffy, C., Berton, N., Sippy, J., Overduin, M., Feiss, M. and Catalano, C.E. (2002) Mol. Cell 9, 981–991.